Environ Sci Pollut Res (2013) 20:7534–7549
DOI 10.1007/s11356-013-1495-2

Quantitative–spatial assessment of soil contamination in S. Francisco de Assis due to mining activity of the Panasqueira mine (Portugal)

Eduardo Ferreira da Silva · Paula Freire Ávila · Ana Rita Salgueiro · Carla Candeias · Henrique Garcia Pereira

Received: 13 October 2012 / Accepted: 15 January 2013 / Published online: 31 January 2013

Abstract Through the years, mining and beneficiation processes produces large amounts of As-rich mine wastes laid up in huge tailings and open-air impoundments (Barroca Grande and Rio tailings) that are the main source of pollution in the surrounding area once they are exposed to the weathering conditions leading to the formation of AMD and consequently to the contamination of the surrounding environments, in particularly soils. In order to investigate the environmental contamination impact on S. Francisco de Assis (village located between the two major impoundments and tailings) agricultural soils, a geochemical survey was undertaken to assess toxic metals associations, related levels and their spatial distribution, and to identify the possible contamination sources. According to the calculated contamination factor, As and Zn have a very high contamination factor giving rise to 65.4 % of samples with a moderate to high pollution degree; 34.6 % have been classified as nil to very low pollution degree. The contamination factor spatial distribution put in evidence the fact that As, Cd, Cu, Pb, and Zn soils contents, downstream Barroca Grande tailing, are increased when compared with the local Bk soils. The mechanical dispersion, due to erosion, is the main contamination source. The chemical extraction demonstrates that the trace metals distribution and accumulation in S. Francisco de Assis soils is related to sulfides, but also to amorphous or poorly crystalline iron oxide phases. The partitioning study allowed understanding the local chemical elements mobility and precipitation processes, giving rise to the contamination dispersion model of the study area. The wind and hydrological factors are responsible for the chemical elements transport mechanisms, the water being the main transporter medium and soils as one of the possible retention media.

Keywords Soil contamination · Principal component analysis (PCA) · Correspondence analysis (CA) · Availability · Panasqueira mining area

Responsible editor: Zhihong Xu

E. Ferreira da Silva (✉) · A. R. Salgueiro · C. Candeias
Geosciences Department, Geobiosciences, Geotechnologies and Geoengineering (GeoBioTec) Research Center, University of Aveiro, Campus de Santiago, 3810-193 Aveiro, Portugal
e-mail: eafsilva@ua.pt

P. Freire Ávila
LNEG–National Laboratory of Energy and Geology. S. Mamede Infesta INETI, 4466-956 S. Mamede de Infesta, Portugal

H. Garcia Pereira
Technical Institute, CERENA–Technical University of Lisbon, Avenida Rovisco Pais, 1, 1049-001 Lisboa, Portugal

Introduction

Metal mining processing and smelting have been recognized as a major contributor to environmental pollution, providing sources of heavy metals that may lead to the contamination of the surrounding environment (Adriano 1986; Benvenuti et al. 1995; Gray 1997; Liu et al. 2003; Zhou et al. 2007). High concentrations of heavy metals can be found in and around abandoned and active mines due to the discharge and dispersion of mine waste materials into nearby soils, food crops, and stream sediments (Lee et al. 2001; Jung 2001; McKenzie and Pulford 2002; Witte et al. 2004). This will eventually lead to a loss of biodiversity, amenity, and economic well being, and a potential health risk to residents in the vicinity of the mining area may occur (Verner and Ramsey 1996; Lee et al. 2001; Wong et al. 2002; Galán et al. 2003).

At present, management of contaminated soils is a major issue, which may have serious consequences. Numerous

chemical compounds, organic and inorganic, are usually toxic and so it becomes necessary to assess their adverse impacts on human health and on the environment. Also, the extent and magnitude of the risk posed by such chemicals, and what cleanup goals are required for such soils, is a matter of concern.

Metals (and metalloids) such as arsenic (As), cadmium (Cd), chromium (Cr), lead (Pb), or mercury (Hg) are among the most toxic for humans, especially for children (as well as for animals), and can even lead to death if ingested in large doses or over large periods of time. Exposure to these harmful elements may have different pathways, either indirect, through the ingestion of vegetables grown in contaminated soils or direct ingestion of soil (geophagy; Ellickson et al. 2001). Geophagy includes dust inhalation and dust ingestion, fueled by its adherence to hands and plants, which may reach human's mouth. This issue leads to exposure to immobile or weakly mobile metals that otherwise would not pose any kind of risk to humans or animals.

These complex sets of processes can be illustrated with the case study of the active Panasqueira mine. The Panasqueira hydrothermal mineralization, located geographically in the municipalities of Covilhã and Fundão (Castelo Branco district, Central Portugal; Fig. 1a) is the biggest Sn-W deposit of Western Europe and has been in operation since 1896 to the present date (Smith 2006).

The paragenesis is complex; nevertheless, four stages of mineral formation are generally accepted by most of the authors who have studied this deposit: (1) oxide silicate phase [quartz, wolframite, and cassiterite]; (2) main sulfide phase [pyrite, arsenopyrite, pyrrothite, sphalerite, AND chalcopyrite]; (3) pyrrothite alteration phase [marcasite, siderite, galena, and Pb-Bi-Ag sulphosalts]; (4) late carbonate phase [dolomite and calcite] (Breiter 2001; Corrêa de Sá et al. 1999; Correa and Naique 1998; Noronha et al. 1992; Cavey and Gunning 2006). At Panasqueira, more than 65 minerals including sulfides, sulphosalts, oxides, carbonates, silicates, phosphates, and tungstates minerals have been identified (Kelly and Rye 1979).

The mining and beneficiation processes at the site produces metal-rich mine wastes, being Barroca Grande≈ 7 Mm^3 with two mud dams≈1.2 Mm^3 (one of these dams still active while the older one is deactivate) one of the main deposits in the mine area. According to Ávila et al. (2008), the rejected materials from the ore processing, containing high concentrations of metals, are stored in the open-air impoundments. Barroca Grande impoundment shows high concentrations of As, Cd, Cu, and Zn (Ávila et al. 2008; e-Ecorisk 2007). The unconfined tailings and open impoundments are the main source of pollution in the surrounding area once the oxidation of sulfides can result in the mobilization and migration of trace metals from the mining wastes into the environment, releasing contaminants into the ecosystem. The effect of Panasqueira mining activities and the metals release from acid mine waters to ground waters and stream sediments is dynamic and actual. Soils, downstream Barroca Grande tailing, will be a major repository for the heavy metals released with the S. Francisco de Assis village the most affected.

In this paper, the environmental contamination impact on S. Francisco de Assis (SFA) agricultural and urban soils due to the mining activities is investigated. The objectives of the study are (a) to assess the levels of soil contamination in respect to average concentrations of toxic metals in the region, (b) to determine the associations between the different toxic elements and their spatial distribution, and (c) to identify possible sources of contamination that can explain the spatial patterns of soil pollution in the SFA.

Materials and methods

Field sampling

The soil sampling collection was established according the site-specific characteristics. In the study area, the soil is mostly an incipient and lithic soil derived from a metasediments substrate (cambisols), and therefore the depth of sampling was set to a maximum of 10 cm to guarantee that all samples could be collected at the same conditions. A total of 75 soil samples were collected downstream Barroca Grande tailing (SFA1 to SFA75; Fig. 1b and c) in the vicinity of SFA. To establish the local geochemical background, 20 unaffected soil samples (SoBK1 to SoBK20; Fig. 1b) were also collected outside of the contaminated area (Casegas area). All samples have been georeferenced to Universal Transverse Mercator coordinates. Soil samples were dried at 40 °C in an oven, homogenized and sieved through a <200 mesh screen in order to prepare them for chemical analysis.

Sample chemical analysis

The <200 mesh soil fractions were submitted to multielemental analysis in the S. Mamede de Infesta (LNEG) accredited lab. For trace metal analysis, a 0.5 g split was leached in hot (95 °C) aqua regia (HCl-HNO_3-H_2O) for 1 h. After dilution to 10 ml with water, the solutions were analyzed for 22 chemical elements by conductive plasma emission spectrometry (Ag, As, B, Ba, Be, Cd, Co, Cr, Cu, Fe, Mn, Mo, Nb, Ni, P, Pb, Sb, V, Y, and Zn) and X-ray (Sn, W). The detection limits were based on three times the standard deviation of a blank reagent that was analyzed

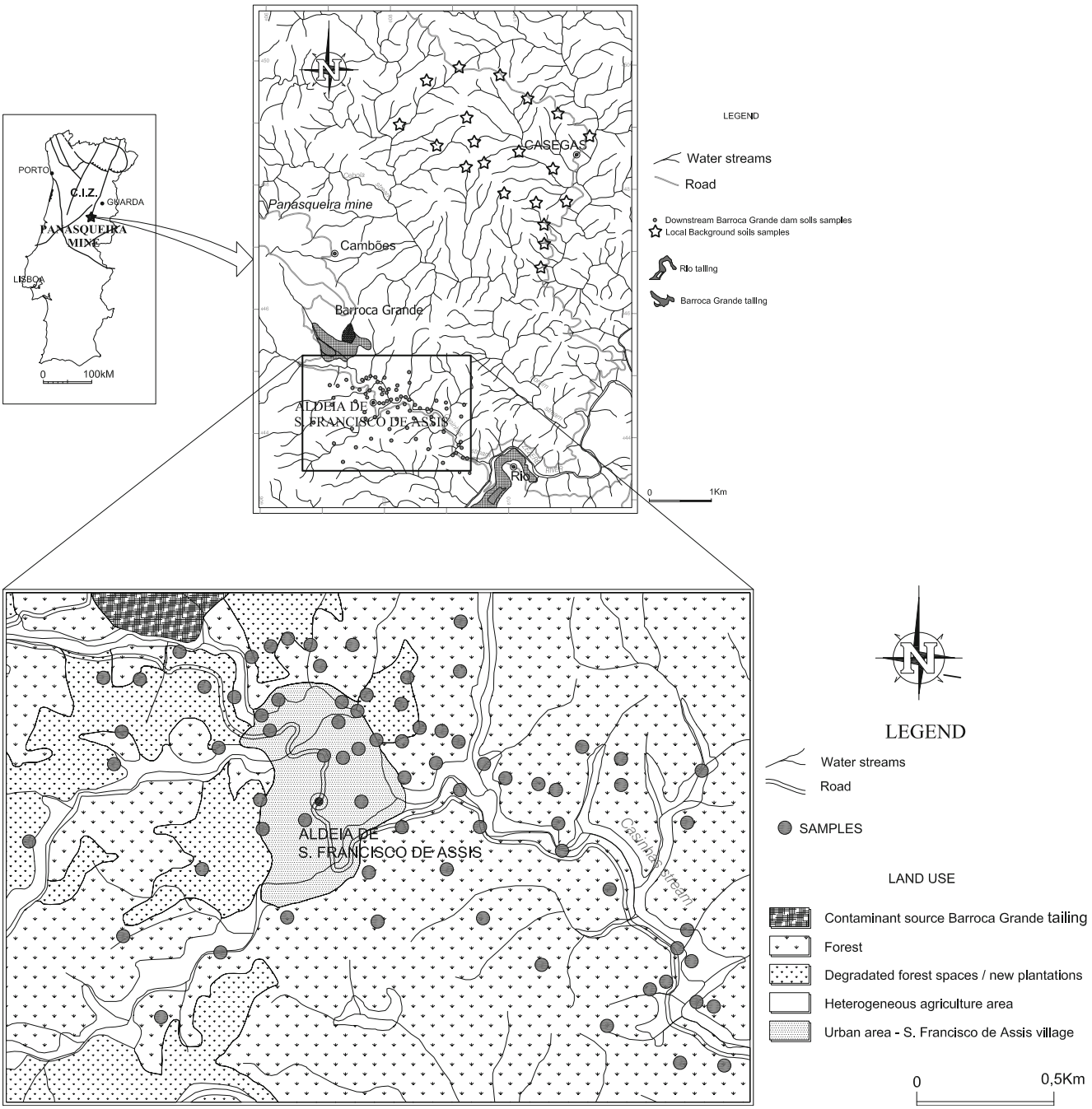

Fig. 1 **a** Panasqueira mine location, **b** sampling location of soil samples including background samples (Casegas area), **c** synthetic map showing the location of S. Francisco de Assis study area, including sampling location and land use codes

ten times. Accuracy and analytical precision were determined using analyses of reference materials (SO1, SO2, SO3, SO4, FER1, FER2, FER3, FER4 from Canadian Centre of Mineral and Energy Technology; PACS-1 from NRS26 CNRC; 2711 from NIST) and duplicate samples in each analytical set. The results were within the 95 % confidence limits of the recommended values given for this certified material. The relative standard deviation was between 5 and 10 %.

Mineralogical studies

The mineralogical characterization in selected soil samples included: (1) reflected and light optical microscope identification and (2) X-ray diffraction (XRD) using a Philips difractometer (model X'Pert). Working conditions were automatic divergence slit, Cu Kα monochromatic radiation, graphite monochromator, 20 mA and 40 kV. Samples were run at a speed of 0.05° 2θ/min (2–70°). The mineral

constituents (including efflorescence) were identified by X-ray diffraction at LNEG.

Selective chemical extraction procedure

The fine-grained fraction (<200 mesh) of two representative samples (SFA3 and SFA18) was submitted to sequential chemical extraction (SCE) procedure in ACTLABS (Ontario, Canada), accredited under ISO 9001 and 9002. Reagents were applied sequentially according to their chemical aggressivity. The extractable fractions were obtained by extraction with different solutions: (a) F_1—sodium acetate (NaOAc, pH5) for extraction of exchangeable cations adsorbed by clay and those soluble in water or in slightly acidic conditions and coprecipitated by carbonates (the most labile bonded and therefore the most dangerous and bioavailable for the environment); (b) F_2—cold hydroxylamine for extracting amorphous Fe oxides and crystalline Mn oxides (metals bound to Fe and Mn oxides that can be released if conditions change from oxic to anoxic state); (c) F_3—hot hydroxylamine for extraction of amorphous and crystalline Fe oxides and crystalline Mn oxides; (d) F_4—aqua regia, for leach sulfide species (metals which may be released under oxidizing conditions) and clay minerals; (e) F_5—four acids digestion (or total attack) where metals strongly associated with crystalline structures of minerals (such as the remaining silicates) will be decomposed (they are therefore unlikely to be released).

The recovery of the sequential extraction procedure for Ag, As, Cd, Co, Cr, Cu, Fe, Mn, Ni, Pb, Sn, W, and Zn was calculated (Eq. 1) by comparing the sum of the five fractions from the SCE with the total amount obtained after hot mixed acid attack of the same sample as follows:

$$\text{Recovery}(\%) = [(F_1 + F_2 + F_3 + F_4 + F_5)/\text{total concentration}] \times 100 \quad (1)$$

For all elements, the total of the trace elements in the different fractions did not exceed ±10 % of the bulk sample which is accepted as satisfactory (Tessier et al. 1979; Pickering 1986; Yan et al. 1999).

The relative extraction ratio (RER) was also calculated (Eq. 2) by the ratio between the element concentration extracted by the individual leaching (CIL) procedure and the concentration extracted by total attack (CTA; Son and Jung 2011) as follow:

$$\text{Relative extraction ratio}(\%) = \left[\text{CIL}\ \left(\text{mg kg}^{-1}\right)/\text{CTA}\ \left(\text{mg kg}^{-1}\right)\right] \times 100 \quad (2)$$

Data analysis

Principal component analysis (PCA) and correspondence analysis (CA) In this study, PCA was performed to decrease the dimension of the space where variables are projected (Einax and Soldt 1999; Massart and Kaufman 1983). The number of significant principal components for interpretation was selected on the basis of the Kaiser criterion, which consists of retaining those factors where eigenvalue is higher than 1 (Davis 1986; Manly 1994) and gives rise to a total of explained variance equal or higher than 70 %.

Once identified, the contaminant group of elements associated with ore exploitation and processing, a complete disjunctive matrix of the data was built classifying each sample, for each element according to a set of rules. If a sample value is below the average value of local background (Casegas soils), the sample is considered clean (the label of the element contains a C). If the sample is above literature guideline values for agriculture purposes, it is considered to require a sort of remediation/reclamation (the label of the element contains an R). On the other hand, if sample value is between average local background and guideline value, it is considered to be in need of intervention, i.e., further investigation is required (the label of the element contains an I). Regarding guideline values for Portuguese agricultural soils, Ferreira (2004) established the following limits: As=30 $mgkg^{-1}$, Co=40 $mgkg^{-1}$, Cu=100 $mgkg^{-1}$, Ni=75 $mgkg^{-1}$, and Zn=300 $mgkg^{-1}$. These values were used as the lower limit of a soil requiring reclamation. For Be (4 $mgkg^{-1}$), Cd (4 $mgkg^{-1}$), and Pb (70 mg kg^{-1}), the limits used were the ones established by the Canadian Council of Ministers of the Environment (CCME; 1999) guidelines for agriculture soils, even though these limits do not refer specifically to Portuguese soils. Neither Ferreira (2004) nor CCME (1999) present guideline values for Y, Sn, and W, and so only two categories were established for such elements: inferior or superior to average local background (the last case being considered as requiring further investigation). The referred complete disjunctive matrix was then submitted to a CA. Since CA allows to project variables and samples in the same factorial space (Greenacre 1984), it is possible to extract a hierarchy of samples according to their contamination level. PCA and CA analysis were performed using Andad (v.7.12) software (Andad 2000).

Spatial estimation In order to produce maps of spatial distribution of chemical elements concentrations and contamination factors, a variographic study followed by ordinary kriging (OK) was performed (Goovaerts 1997; Wackernagel 1998). Variograms were constructed and modeled with geoMS software (geoMS 2000), the estimation, by ordinary kriging, was also performed with geoMS software. Maps were produced with ArcGis (v. 9.3) software.

Enrichment index calculation In order to evaluate the degree of trace metal contamination in soils, an enrichment index (Nishida et al. 1982; Chon et al. 1995; Kim et al. 1998; Ferreira da Silva E et al. 2005) was computed by averaging the ratios of the element concentration (in milligram per kilogram) to the median values of the background samples.

Contamination factor and modified degree of contamination This is based on the calculation for each pollutant of a contamination factor (C_f; Hakanson 1980). C_f (Eq. 3) is the ratio obtained by dividing the mean concentration of each metal in the soil (C_i) by the baseline or background value of the specific metal (C_b; Liu et al. 2005):

$$C_{f=}\ C_i/C_b \text{ and } C_d = \left(\sum\nolimits_{1=1}^{i-n} C_f^i\right) \quad (3)$$

C_f is defined according to four categories as follows (Liu et al. 2005): C_f<1—low contamination factor; 1<C_f <3—moderate contamination factor; 3<C_f <6—considerable contamination factor; C_f>6—very high contamination factor.

Abrahim and Parker (2008) presented a modified and generalized form of the Hakanson (1980) equation for the calculation of the overall degree of contamination as below (Eq. 4).

$$\mathrm{mC_d} = \left(\sum\nolimits_{1=1}^{i=n} \mathrm{C_f^i}\right)/\mathrm{n} \quad (4)$$

where:n=number of analyzed elements and i=ith element (or pollutant) and C_f=contamination factor.

For the classification and description of the modified degree of contamination (mC_d) in soil, the following gradations are proposed: mC_d<1.5—nil to very low degree of contamination; 1.5<mC_d<2—low degree of contamination; 2<mC_d <4—moderate degree of contamination; 4<mC_d<8—high degree of contamination; 8<mC_d<16—very high degree of contamination; 16<mC_d<32—extremely high degree of contamination; mC_d>32—ultrahigh degree of contamination (Abrahim and Parker 2008).

Results and discussion

Basic statistical analysis

Descriptive statistics for the aqua regia extracted fraction of Ag, As, B, Ba, Be, Cd, Co, Cr, Cu, Fe, Mn, Mo, Nb, Ni, P, Pb, Sb, Sn, V, W, Y, and Zn for both SFA and Casegas soils are given in Table 1. According to the results, it can be noticed that SFA shows higher mean values for As, Ag, As, B, Cd, Cr, Cu, Mn, Mo, Ni, P, Sn, W, Y, and Zn when compared to Casegas values (Table 1).

Comparing the results for both areas, there are some elements that stand out due to differences in its contents. The maximum value of As is 24 times bigger in SFA soils than in Casegas soil samples. The same occurs for other elements, such as: Cd (16.5×), Co (16.9×), Cu (14×), Mn (37.5×), Sn (15×), and W (42×). Soil samples of SFA are enriched with As, Cd, Cu, Mn, and Zn by comparison to reference values for world unpolluted soils (Table 1), while Casegas soils contain low concentrations of As, Cu, Mn, Pb, Sb, and Zn. According to Reimann and De Caritat (1998) and Deschamps et al. (2002), As, Cd, Cu, and Zn mean concentrations in world unpolluted top soils are 5, 0.3, 25, and 70 mgkg^{-1}, respectively, while the respective mean values for soils of the SFA are 118, 2.2, 122, and 388 mg kg^{-1}. Also, the same elements exceed the mean values proposed for Portuguese soils (MPS, Table 1), the values proposed for cambisols (Table 1) and podzols (Table 1; Ferreira 2004).

PCA analysis and geochemical interpretation

A matrix of 95 (samples)×22 (chemical elements) was submitted to a PCA giving rise to the extraction of six principal components which explains 84.81 % of the total variance (Table 2). The first two factorial planes (Fig. 2) account for 67.13 % of total variance and explain all variables with exception of P, associated with the negative PC4 (−0.6166, loading value; see Table 2) and Mo, associated with the positive semi-axis 6 (0.5810, loading value; see Table 2).

The plot of the PCA results (Fig. 2) show the position of the selected 22 variables coordinates, representing the correlation coefficients between them in the different factorial plans. Four groups of variables can be identified in the two most important factorial plans.

The first factorial plan (PC1/PC2) contains 57.63 % of the global information of the dataset. The PC1, which explains 43.38 % (Table 2) of the total variance is associated to Cu, Y, Co, Mn, Cd, As, Zn, Ni, Be, W, Sn, and Pb (group A). Correlation coefficients values indicate strong association of the following pairs: As–W (r=0.83, p<0.05), As–Cu (r=0.84, p<0.05), Co–Fe (r=0.86, p<0.05), Co–Ni (r=0.88, p<0.05), Cu–W (r=0.80, p<0.05) and Sn–W (r=0.80, p<0.05), and also Co–Zn, As–Cd, and Ni–Zn (r=<0.8, p<0.05).

In group A, two subsets of associations are revealed: (a) one with negative loadings in PC1 and positive loadings in PC2 (A_1—As, Sn, W, Cu, and Y) which seems to be controlled by the mixed sulfide mineralization since all the elements summarized by this factor are characteristic of the sulfide ore chemistry in the area representing the residual contamination within the study area; (b) other subset exhibits negative loadings in PC1 and PC2 (A_2—Be, Cd, Co, Mn, Pb, Zn, and Ni) is identified indicating that the

Table 1 Descriptive basic statistics (mean, median, minimum, maximum, and skewness) for selected chemical elements in SFA and Casegas soils (all values are expressed in milligrams per kilogram except for Fe expressed in percent)

	DL	Data from literature							S. Francisco de Assis (n=75)					Casegas area (n=20)				
		MWS	NRS	MCNS	MPS	CBS	PZS	GVPS	Mean	Mdn	Min	Max	Skw	Mean	Mdn	Min	Max	Skw
Ag	1	–	–	–	0.2	–	–	–	1.0	1.0	1.0	3.0	8.66	1.0	1.0	1.0	1.0	N/A
As	20	5	0.1–40	40	11	17	3	22	118	82	9	831	3.47	14	9	9	34	1.47
B	8	–	–	–	2	–	–	–	71	38	6	476	2.82	25	25	8	47	0.56
Ba	25	500	90–300	–	53	46	27	53	289	292	149	414	−0.28	338	335	233	574	2.05
Be	1	–	–	–	–	–	–	–	2.2	2.0	1.0	8.0	1.96	2.2	2.0	1.0	3.0	0.00
Cd	4	0.3	0.01–2	0.7	0.1	–	–	0.2	4.1	2.0	2.0	33.0	3.37	2.0	2.0	2.0	2.0	N/A
Co	9	10	0.5–65	30	8	6	2	8	19	10	5	169	4.05	10	10	10	10	N/A
Cr	8	80	5–1,500	150	21	16	6	21	206	198	131	326	0.90	148	149	116	209	1.52
Cu	1	25	2–250	100	16	13	6	16	122	72	23	791	3.05	37	35	17	57	0.17
Fe	0.2	5.00	1.00–10.00	–	2.74	2.54	0.69	–	3.98	3.90	2.40	7.00	1.57	4.54	4.40	3.70	5.60	0.41
Mn	50	700	20–10,000	2,000	393.5	251	154	–	1,169	275	80	20,000	4.83	297	307	111	534	0.37
Mo	4	1.2	0.1–40	4	0.5	–	–	1	2.2	2.0	2.0	11.0	6.14	4.0	4.0	4.0	4.0	N/A
Nb	4	–	–	–	–	–	–	–	9.7	10.0	2.0	15.0	−0.18	12.3	12.0	9.0	18.0	0.89
Ni	13	20	2–750	80	16	10	3	16	41	19	7	472	5.81	20	19	19	39	4.45
P	30	–	–	–	380	490	140	–	857	550	227	4,197	2.26	558	493	330	1,016	1.35
Pb	16	17	2–300	100	21	24	16	21	24	16	8	78	1.56	22	16	16	57	2.02
Sb	12	–	–	–	1.5	–	–	–	8.6	10.0	6.0	19.0	0.84	10.0	10.0	10.0	10.0	N/A
Sn	6	–	–	–	–	–	–	–	30	17	6	167	2.31	6	6	4	11	1.18
V	6	90	3–500	200	27	28	11	27	102	101	59	139	0.21	122	124	98	143	−0.56
W	18	–	–	–	1	–	–	–	63	37	3	592	3.82	6	5	2	14	1.46
Y	1	–	–	–	–	–	–	–	14.8	9.0	3.0	95.0	3.09	4.9	5.0	3.0	7.0	0.08
Zn	5	70	1–900	300	54.5	61	14	55	388	273	100	2,709	3.73	258	262	210	299	−0.29

DL detection limit of the method, *MWS* mean world soils (according to Deschamps et al. (2002), Reimann and De Caritat (1998)), *NRS* normal ranges in soils (according to Radojevic and Bashkin (1999)), *MCNS* maximum content in normal soils (according to Henin (1983) and Godin (1983)), *MPS* median values for Portuguese Soils (Ferreira 2004), *CBS* mean values for Portuguese Cambissols (Ferreira 2004), *PZS* mean values for Portuguese Podzols (Ferreira 2004); *GVPS* guideline values for Portuguese soils (Ferreira 2004), *Mdn* median value

Table 2 Factor loadings of each variable, variance, explained and cumulative variance of the PC

	PC1	PC2	PC3	PC4	PC5	PC6
Ag	−0.4714	0.0710	−0.6637	0.0841	−0.4658	−0.1456
As	−0.8986	0.1088	−0.1509	−0.0071	−0.1493	−0.0896
B	−0.3294	0.1936	−0.5234	−0.4006	0.5588	0.2313
Ba	−0.1103	−0.6658	0.0520	−0.4612	−0.0310	−0.1838
Be	−0.8324	−0.2801	−0.1806	−0.1857	0.1701	0.0846
Cd	−0.9142	−0.1136	0.1398	0.2349	0.0457	−0.0142
Co	−0.9440	−0.1214	0.1753	0.1999	0.0671	−0.0027
Cr	−0.1083	0.6484	0.0861	−0.0371	0.1025	−0.5152
Cu	−0.9713	0.0156	−0.0202	0.0869	−0.0676	−0.0283
Fe	−0.1024	−0.8024	−0.1548	−0.0872	−0.0539	−0.2677
Mn	−0.9183	−0.1323	0.2182	0.2080	0.0968	0.0091
Mo	0.2243	−0.3595	−0.1298	0.4380	−0.1575	0.5810
Nb	0.2789	−0.6432	−0.1468	0.0635	0.2050	−0.0935
Ni	−0.8633	−0.1412	0.2929	0.2010	0.1797	0.0075
P	−0.4069	−0.0545	0.2484	−0.6166	−0.4525	0.2332
Pb	−0.5301	−0.1112	0.2017	−0.3424	−0.4275	0.1094
Sb	0.1664	−0.0710	−0.7666	0.3206	−0.1900	−0.0493
Sn	−0.6275	0.1779	−0.4248	−0.3575	0.3681	0.1606
V	0.2567	−0.8649	−0.1317	−0.0192	0.0966	−0.1788
W	−0.8012	0.2336	−0.3611	0.0165	−0.2034	−0.0624
Y	−0.9711	0.0130	−0.0228	0.0954	−0.0675	−0.0281
Zn	−0.8788	−0.1753	0.2090	0.2048	0.1884	0.0090
Eigenvalue	9.54	3.13	2.09	1.59	1.36	0.94
Explained variance (%)	43.38	14.25	9.50	7.21	6.20	4.27
Cumulative variance (%)	43.38	57.63	67.13	74.34	80.54	84.81

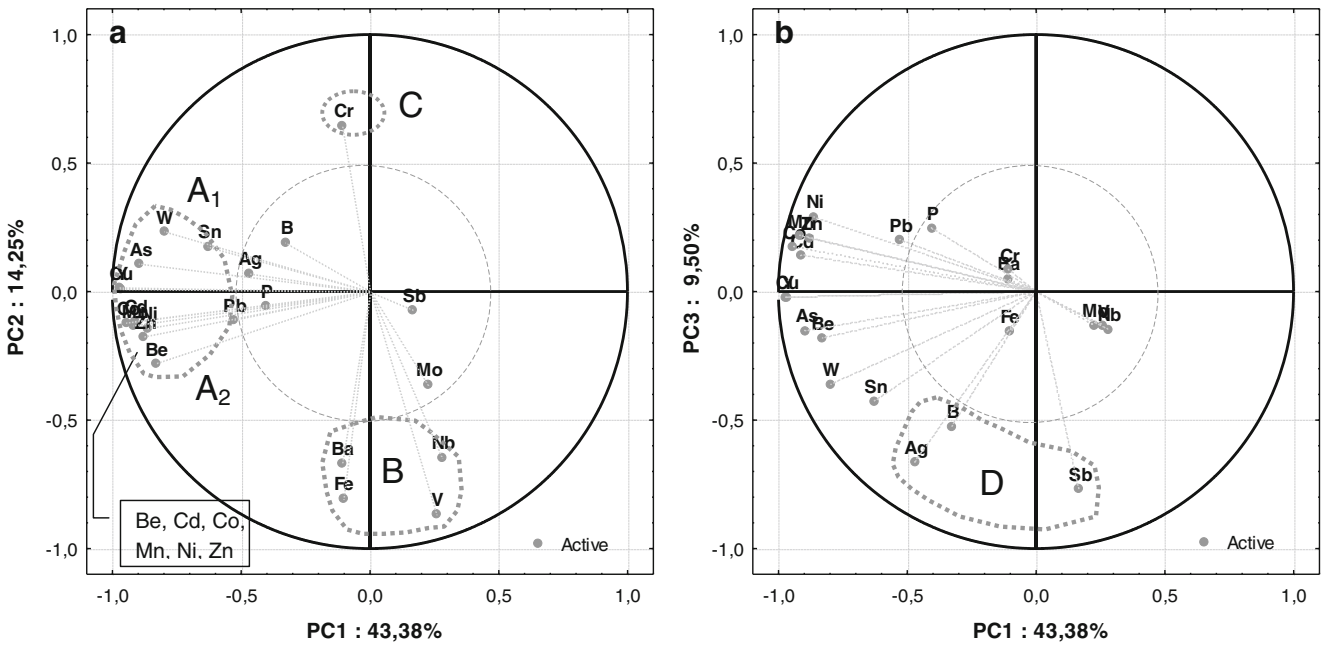

Fig. 2 Graphical representation of the first two factorial planes of PCA

representative elements of the original paragenesis (such as wolframite (Fe,Mn)WO_4), pyrite (FeS_2), pyrrhotite ($Fe_{(1-x)}S$ (x =0–0.2)), arsenopyrite (FeAsS), chalcopyrite ($CuFeS_2$), cassiterite (SnO_2), beryl ($Be_3Al_2(Si_6O_{18})$, mica, and fluorite (CaF_2)) still maintain a close relationship in the secondary environment. The association As, Sn, and W represents the oxide–silicate mineral formation phase (quartz, wolframite, and cassiterite), while the associations Cu and Y, and Be, Cd, Co, Mn, Pb, Zn represents the main sulfide phase (pyrite, arsenopyrite, pyrrothite, sphalerite ((Zn,Fe)S), and chalcopyrite) and the pyrrothite alteration phase [marcasite (FeS_2), siderite ($FeCO_3$), galena (PbS), and Pb-Bi-Ag sulphosalts].

These associations reflect the strong influence of the Rio and Barroca tailings and mud dams. According to Ávila et al. (2008), the Rio tailings samples contain scorodite ($FeAsO_4 \cdot 2H_2O$), sphalerite, wolframite, quartz, natrojarosite ($NaFe^{3+}3(SO_4)2(OH)_6$), montmorilonite ((Mg,Ca)O.$Al_2O_3Si_5O_{10}.nH_2O$), vermiculite($(Mg,Fe,Al)_3(Al,Si)_4O_{10}(OH)_2.4H_2O$), ilite, some silicates like kaolinite ($Al_2Si_2O_5(OH)_4$), and also sulfate minerals. In contrast, in the Rio tailings dam, melanterite ($Fe^{2+}(SO_4).7(H_2O)$) and minor amounts of rozenite ($Fe^{2+}(SO_4).4(H_2O)$) and szomolnokite ($Fe^{2+}(SO_4).(H_2O)$) are present. The Rio dam consists predominantly of quartz, mica, feldspar, illite–vermiculite, arsenopyrite, marcasite, pyrite, pyrrhotite, and chalcopyrite. Other minerals, like scorodite and natrojarosite, are also present. The DRX analysis of the active dam sample of Barroca Grande revealed the presence of scorodite, arsenopyrite, quartz, sphalerite, heamatite (Fe_2O_3), and muscovite ($KAl_2(AlSi_3O_{10})(F,OH)_2$) while the sample from the old dam of Barroca Grande contained quartz, pyrite, chalcopyrite, wolframite (ferberite), and scorodite (Ávila et al. 2008). The samples collected in the tailing materials of Barroca Grande consist predominantly of arsenopyrite, wolframite (ferberite), quartz, and muscovite.

The PC2, which explains 14.25 % of the total variance, is related with two groups (group B, associated to the negative scores—Fe-Ba and Nb-V; group C, associated with the positive scores—Cr). PC2 can be associated with the dominant lithological unit (brown argilaceous schists and dark gray siliceous schist interbedded with rare greywackes). Few mafic rocks (dolerites) were observed, particularly near S. Jorge da Beira (NW–SE subvertical).

The second factorial plan (PC1/PC3, representing 52.88 % of total variance) is dominated by the association of Sb, Ag, and B variables (group D). This plan separates the main sulfide minerals phases from the sulphosalts.

Level of soil pollution and environmental quality

A simplified approach to risk assessment was adopted in this study by comparing the measured level of soil contamination in SFA with local geochemical background values (Table 1). PCA results show that As, Cd, Co, Cu, Mn, Ni, Sn, Y, W, and Zn were the elements of most concern. Table 3 shows the results of C_f and the mC_d.

According to the results, the highest C_f values are recorded for As and Zn (median>6.0), while considerable C_f values (3<median <6) occur in Cu, Mn, Y, and Sn. The calculated mC_f values range from 1.1 to 26.4 with an average of 4.0. The cumulative frequency distribution shows that only 34.6 % of the soil samples were classified as nil to very low degree of pollution with mC_d values 2.0, while the remaining 65.4 % exhibit moderate to high degree of pollution (mC_d>2.0). Samples SFA 3 and SFA18 show the highest mC_d values (26.4 and 25.8, respectively). As expected, the Casegas soils are not contaminated or show evidences of low contamination (mC_d=1.1).

In order to assess the spatial distribution of these C_f, experimental variograms were calculated and modeled (Table 4). All variograms, modeled by spherical schemes, show that the nugget effect (C_0) is zero.

Estimation of the spatial distribution of As and Cu was then achieved by OK. The spatial distribution of As (Fig. 3) reveals zones with very high values. Comparison of the SFA data with the MPS values (11 mgkg^{-1}; Table 1) and with the guidelines for agriculture soils in Portugal (30 mgkg^{-1}; Table 1), reveals that 98.6 and 96.3 % are above these values. The mapping of C_f of As highlights that 84.2 % of the study area is classified as high to extremely high contaminated.

The Cu spatial distribution (Fig. 4) also identify high concentrations in the study area. Comparing the Cu values

Table 3 C_f and mC_f using baseline values (median value for Casegas area, considered as representative of geochemical background)

		C_f Ag	C_f As	C_f Cd	C_f Co	C_f Cu	C_f Mn	C_f Ni	C_f Pb	C_f Sb	C_f Sn	C_f W	C_f Y	C_f Zn	mC_f
S. Francisco de Assis	Min	1.0	1.0	1.0	0.5	0.7	0.3	0.3	0.5	0.6	0.6	0.4	1.1	0.6	1.1
	Max	3.0	92.3	16.5	16.9	22.6	65.1	24.8	4.9	1.9	19.0	10.3	30.4	118.4	26.4
	Mdn	1.0	13.1	2.0	1.9	3.5	3.8	2.2	1.5	0.9	3.0	1.5	5.4	12.5	4.0
Casegas	Min	1.0	1.0	1.0	1.0	0.5	0.4	1.0	1.0	1.0	0.6	0.8	0.7	0.4	0.9
	Max	1.0	3.8	1.0	1.0	1.6	1.7	2.1	3.6	1.0	1.4	1.1	2.0	2.8	1.4
	Mdn	1.0	1.5	1.0	1.0	1.0	1.0	1.0	1.4	1.0	1.0	1.0	1.1	1.1	1.1

Table 4 Variogram parameters for each of the studied variables

	Adjusted model function	Main direction (°)	C_0	C_1	Range (m)	Anisotropy ratio
mC_f	Spherical	−65	0	19.71	845	2.19
As	Spherical	−65	0	17,491.00	1,267	2.09
C_fAs	Spherical	−65	0	216.00	1,267	2.32
Cu	Spherical	−65	0	22,363.00	633	1.30
C_fCu	Spherical	−65	0	18.52	633	1.74

In the software used to construct variograms, north direction=0º

with the MPS (16 mgkg^{-1}; Table 1), 98.9 % of the area is above the established threshold. Also, when compared with the guidelines for agriculture soils in Portugal (100 mgkg^{-1}; Ferreira 2004), percentage decreases to 87.1 %. Similarly to As, the mapping of C_f related to Cu variable shows that 81.9 % of the study area is classified as high to extremely high contaminated. For both As and Cu variables, the anomalous areas are located along the Casinhas stream, between Barroca Grande and Rio tailings, in the north area of SFA.

The spatial distribution of mC_d values (Fig. 5) indicate clearly that the highest values occur in soils located near the Rio tailings (area 1), surrounding the Casinhas stream (area 2), and near the Barroca dam materials (area 3; see Table 5).

It must be emphasized that soils collected downstream Barroca Grande tailings show marked increases in the mean concentrations of As (35×), Cd (4×), Cu (4×), Pb (4×), and Zn (22×), compared with background soils. All these values exceed the As, Cd, Cu, and Zn allowed levels (Kloke 1979;

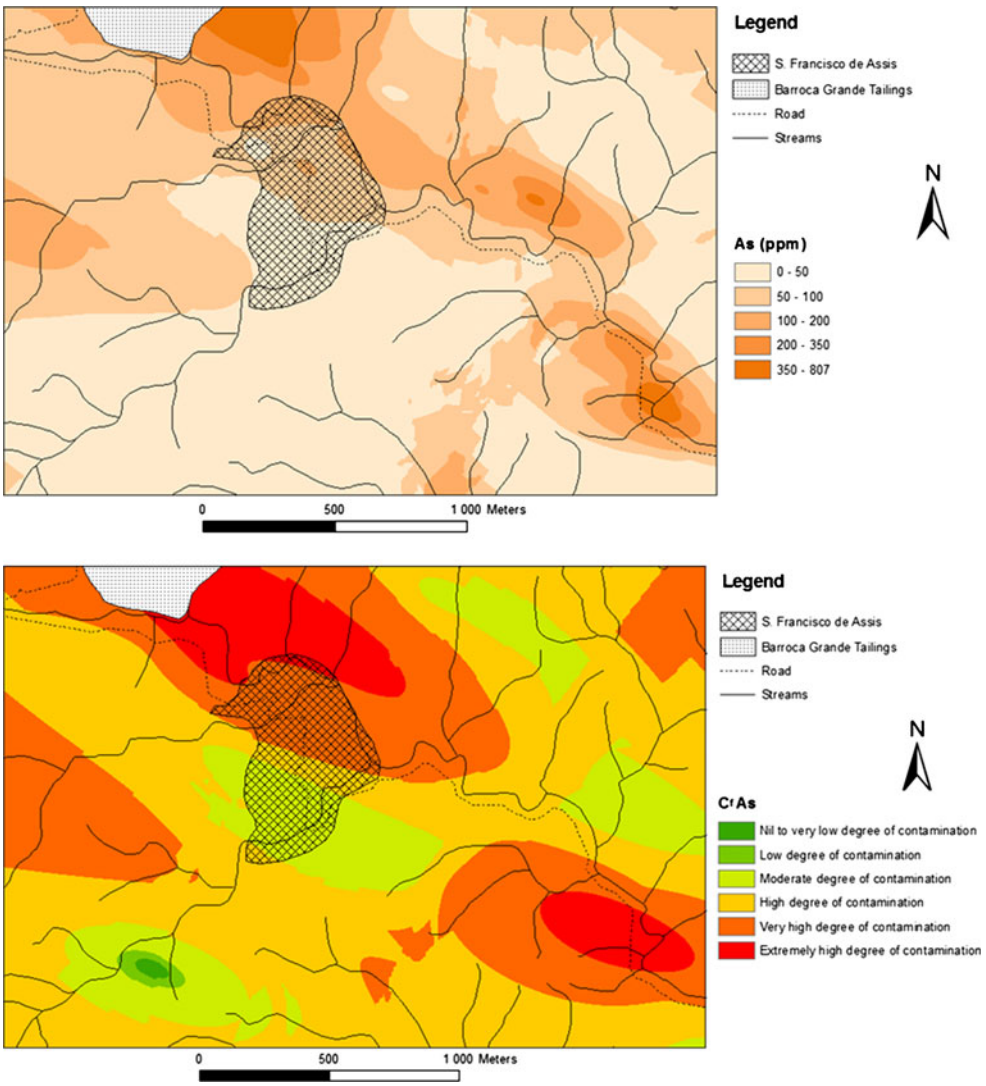

Fig. 3 Spatial distribution of As concentration and related As enrichment factors in S. Francisco de Assis top soils

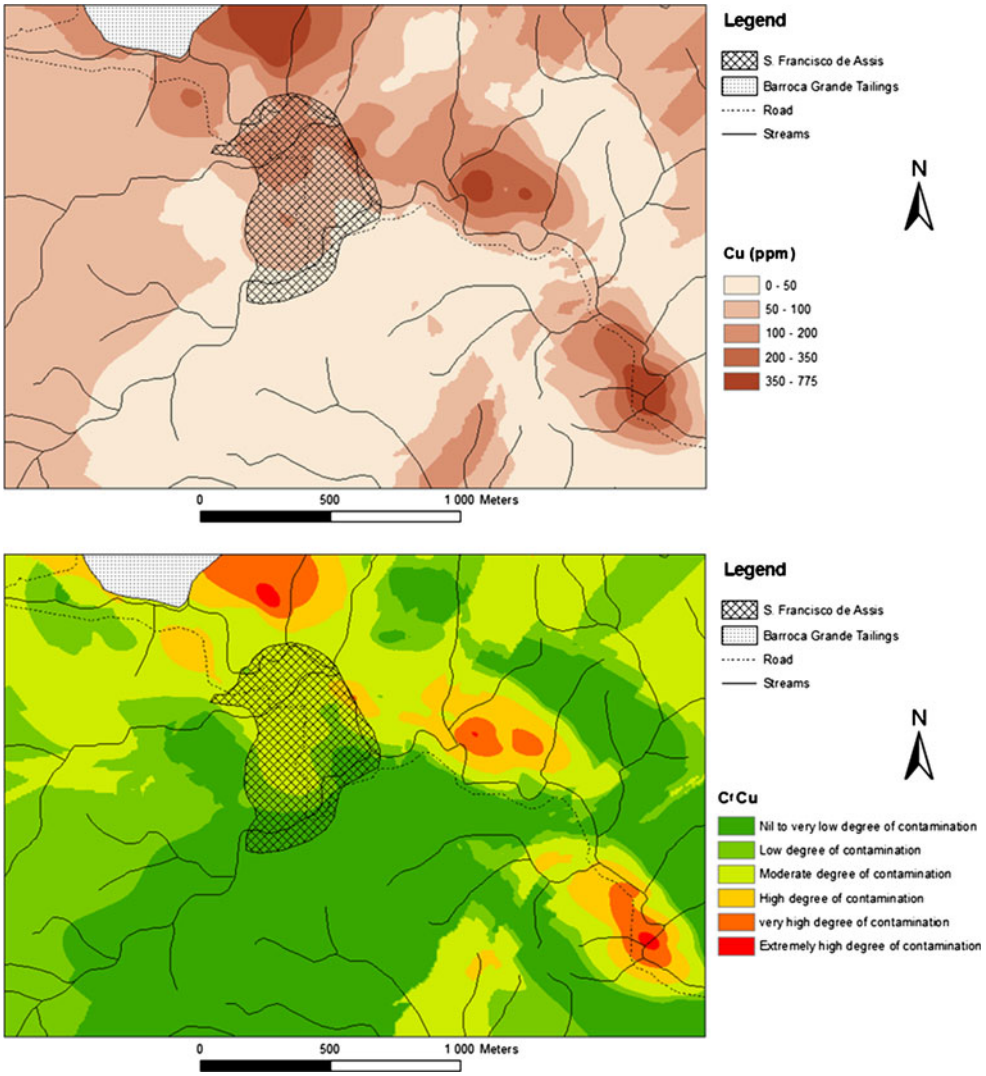

Fig. 4 Spatial distribution of Cu concentration and related Cu enrichment factors in S. Francisco de Assis top soils

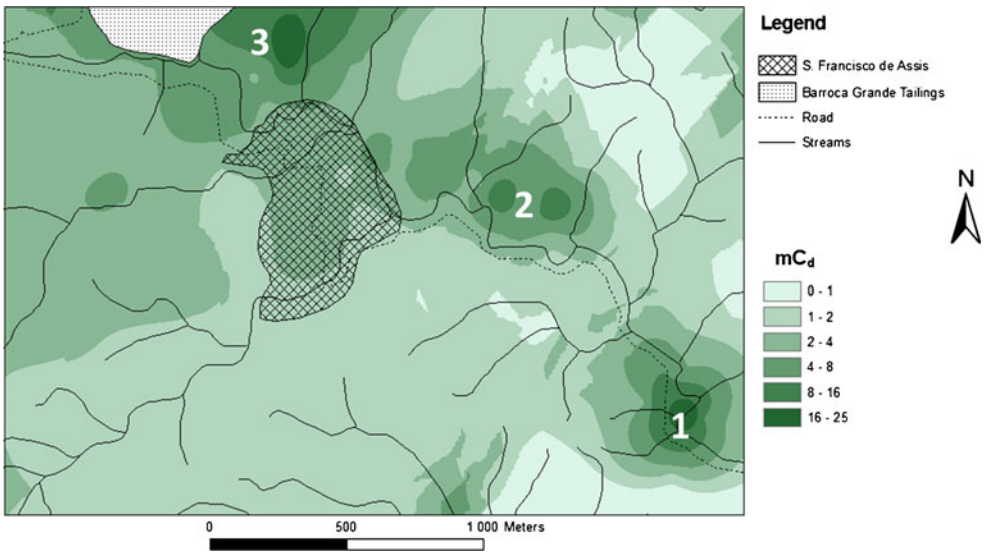

Fig. 5 Spatial distribution of mC_f values in S. Francisco de Assis top soils

Table 5 Average contents for selected chemical elements in soils (all values are expressed in milligram per kilogram except for Fe expressed in percent). Zones 1, 2, and 3 are areas with high values of enrichment index

	D.L.	Zone 1 (N=7)				Zone 2 (N=14)				Zone 3 (N=8)			
		Mean	Mdn	Min	Max	Mean	Mdn	Min	Max	Mean	Mdn	Min	Max
Ag	1	1.3	1.0	1.0	3.0	1.0	1.0	1.0	1.0	1.0	1.0	1.0	1.0
As	20	266	185	73	831	156	128	89	429	257	207	133	697
B	8	80	72	22	228	62	41	24	212	79	57	25	170
Ba	25	267	253	196	336	292	286	189	355	300	317	181	344
Be	1	3.0	2.0	1.0	7.0	2.6	2.0	1.0	5.0	3.1	2.5	1.0	8.0
Cd	4	8.4	2.0	2.0	23.0	6.5	2.0	2.0	31.0	7.8	2.0	2.0	33.0
Co	9	31	10	5	86	29	19	9	107	38	16	10	169
Cr	8	206	193	169	297	211	202	161	314	207	207	143	316
Cu	1	280	161	77	791	185	119	55	622	233	130	94	767
Fe	0.2	4.00	3.80	3.40	4.70	3.96	3.85	3.40	4.60	4.05	4.10	3.30	4.70
Mn	50	2,117	346	226	7,300	2,238	1,107	141	12,000	3,656	849	141	20,000
Mo	4	3.0	2.0	2.0	9.0	2.0	2.0	2.0	2.0	2.0	2.0	2.0	2.0
Nb	4	9.1	9.0	6.0	12.0	8.1	8.5	2.0	13.0	9.6	9.5	6.0	13.0
Ni	13	48	23	18	108	60	46	19	186	97	41	19	472
P	30	934	1,000	408	1,693	1,054	959	349	2,644	1,461	1,416	607	2,907
Pb	16	24	16	8	52	28	25	8	51	44	48	8	78
Sb	12	9.0	6.0	6.0	19.0	6.6	6.0	6.0	10.0	7.0	6.0	6.0	10.0
Sn	6	47	26	19	120	26	18	9	65	53	46	16	112
V	6	92	88	80	110	99	94	85	119	97	99	78	110
W	18	190	134	65	592	81	59	21	267	125	99	40	330
Y	1	33.6	19.0	10.0	95.0	22.2	14.0	7.0	75.0	28.0	16.0	11.0	92.0
Zn	5	541	336	117	1,643	523	283	120	1,705	659	299	165	2,709

Reimann and De Caritat 1998). Also, the W concentrations are higher than 83 mg kg^{-1}.

These high values are probably related to mechanical dispersion of tailing materials as a result of erosion. However, it must be stressed that other mechanisms also contribute to the secondary dispersion of these metals, such as: (a) precipitation of hydroxide, oxyhydroxide, or hydroxysulphate phases from aqueous species as pH increases; and (b) sorption of metals onto neoformed mineral surfaces (carbonates or Fe and Mn coatings, for example), according to Nordstrom (1982) and Chapman et al. (1983).

CA analysis and mapping

The first factorial plane of CA explains approximately 44 % of total inertia of the data. Figure 6a shows that the sequence of ordinal variables follows the axis 1. In fact, lower modalities (considered clean) project onto the negative semi-axis, while greater modalities (requiring reclamation) project onto the positive semi-axis. The modalities are disposed in a parabolic shape (Fig. 6a), showing a clear distribution along the first axis—Guttman effect. Hence, modalities are sequenced in an ascending way along this axis, from clean to requiring reclamation passing through the area of the graph where samples requiring further investigation are project. Asymptotically, this axis can be considered as a proxy of an index of the sample contamination gradient.

Figure 6b presented the projection of the samples in the same factorial plane of Fig. 6a. Samples show the same distribution of modalities along the first axis, allowing identifying which samples are associated with each one of the variable categories.

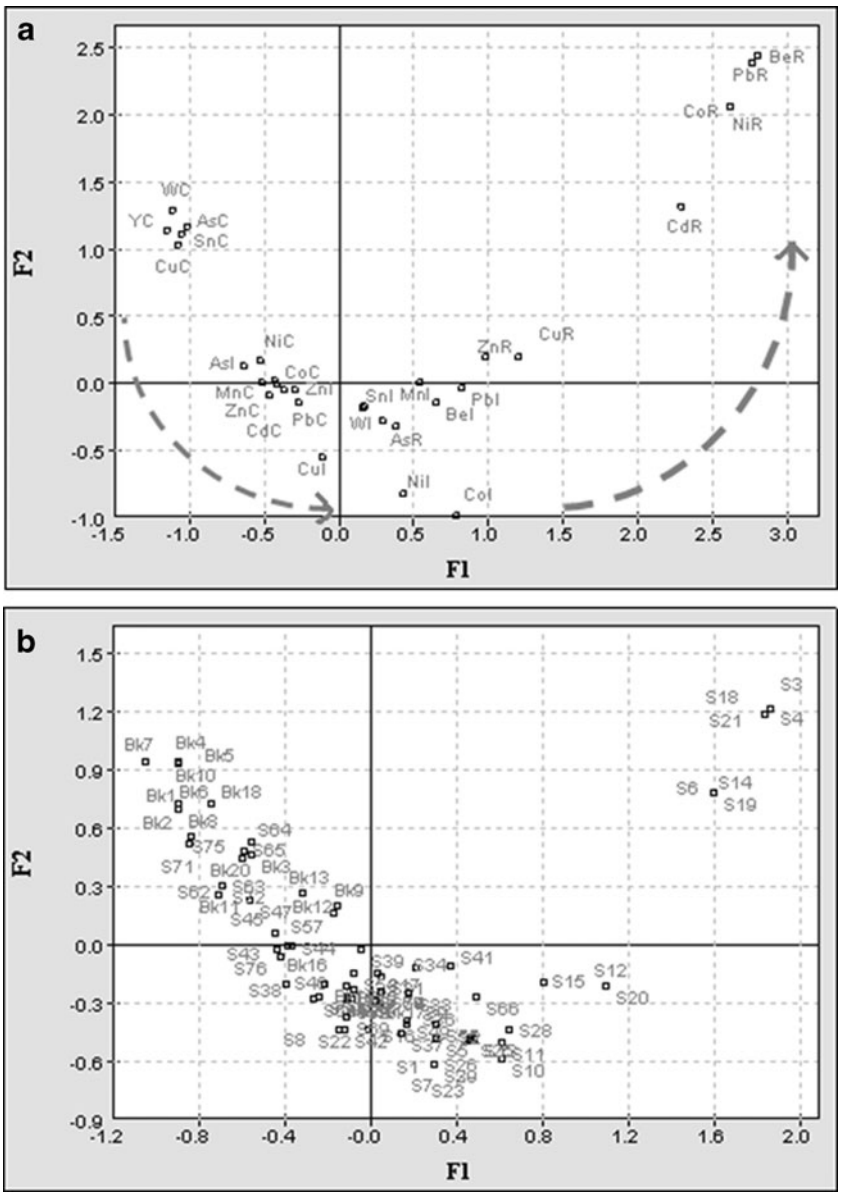

Fig. 6 **a** Graphical representation of modalities projection into the first factorial plane of CA, **b** graphical representation of samples projection into the first factorial plane of CA

In a region where agriculture and cattle breading is, after mining, the principal economic activity, it is imperative to cross-reference the contaminant potential and harmful effect of soils with land use. Figure 7 reveals that samples in need of intervention and reclamation are disposed preferentially in urban and agriculture areas. This fuels the need to perform availability studies in the most pernicious elements in what human health is concerned.

Partitioning of metals in selected samples

The mineralogical study of the two selected soil samples (SFA3 and SFA18—selected according their position in the projection into the first factorial plane of CA; Fig. 6b) by XRD showed that they are composed mainly of quartz, plagioclase, and phylossilicates (biotite, chlorite, muscovite, illite, and kaolinite). However, some iron oxides (haematite, goethite, and magnetite/maghemite) and As (arsenopyrite), Fe (pyrite), Cu (chalcopyrite), Pb (galena), and Zn sulfides (sphalerite) are also present. Iron and Al sulfates (jarosite, $KFe^{3+}3(OH)_6(SO_4)_2$; alunite, $KAl_3(SO_4)_2(OH)_6$) and Fe, Cu, and Pb sulfates and carbonates (siderite, anglesite, malachite, cerusite) are also present. In some samples, plumbugummite ($PbAl_3(PO_4)_2(OH)_5.H_2O$), anidrite ($CaSO_4$), gypsum ($CaSO_4.2H_2O$), and halite (NaCl) are also present.

Using SCE, it was possible to estimate the distribution of Ag, As, Cd, Co, Cr, Cu, Fe, Mn, Ni, Pb, Sb, Sn, W, and Zn among the geochemical fractions on selected soil samples (SFA3 and SFA18), accounting for the relative proportions of each trace metal transported by the mechanical and chemical agents. Table 6 shows the geochemical partitioning of some selected elements in those fractions of each sample.

Iron is mostly extracted by F_4 in the selected soil samples (percent of extraction ranging from 39.2 to 69.3 %), suggesting the presence of sulfides. However, considerable proportion of this metal (up to 50 % in sample SFA3) seems to be also associated to the remaining silicates. It must be pointed out that the percentage of extraction associated to amorphous and crystalline Fe and Mn oxyhydroxides ranges between 8.3 and 9.4 %.

Similar results for As distribution patterns were obtained for the selected soil samples (Table 6). Arsenic seems to be linked to sulfides, since a considerable proportion is extracted by aqua regia (F_4—66.7 to 68.4 %). This high percentage associated with sulfides reflects the presence of arsenopyrite in the samples. Amorphous and crystalline Fe and Mn oxyhydroxides (F_3) seems to be also important metal-bearing phases. The percentage of easily mobilized phases is very low (0.04–0.05 %); however, As concentrations associated with this extraction values (0.4–0.7 mg kg^{-1}) may be considered very high.

Silver, Cd, Co, Cu, Mn, Ni, Pb, and Zn show high (and similar) partitioning patterns in the SFA3 and SFA18 samples (47.7–54.5, 64.8–74.4, 73.4–80.6, 49.5–54.9, 74.4–90.6, 42.4–65.9, 46.2–56.3, and 51–81.1 % of extraction by hydroxylamine leach cold, respectively), suggesting that these may be linked, to some extent, to amorphous Fe/Mn oxyhydroxides. Moreover, part of these elements was extracted with aqua regia in both samples, suggesting that these elements may also be linked, to some extent, to sulfide or clay minerals. It was also shown that Cd (10.3–13.9 % of extraction, 1.9–4 mgkg^{-1} for Cd) and Zn (1.0–2.8 % of extraction, 10–74 mgkg^{-1} for Zn) were also extracted to a great extent with sodium acetate indicating that the soluble/exchangeable/carbonate fraction is probably a preferential sink for Cd and Zn.

These SCE results show that the most pollutant fraction in these soil samples consists of metals bounded to sulfides (such as arsenopyrite, pyrrothite, and chalcopyrite) and released under oxidizing conditions in AMD production processes. Part of this fraction, especially for As, Cd, Cu, and Zn, is temporally retained in solid phases by precipitation of soluble secondary minerals (precipitation of hydrated metal

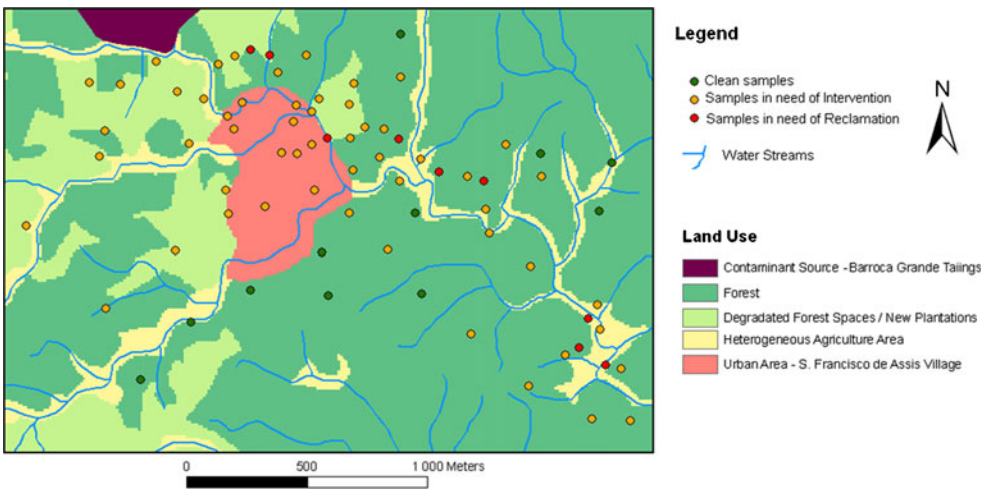

Fig. 7 Sample mapping according to their harmful potential and land use

Table 6 Concentrations (C_{ext}) and RER values of Ag, As, Cd, Co, Cr, Cu, Fe, Mn, Ni, Pb, Sb, Sn, W, and Zn extracted in each step of the sequential extraction procedure (F_1 easily soluble fraction, F_2 amorphous Fe oxides and crystalline Mn oxides, F_3 amorphous and crystaline Fe and crystaline Mn oxides, F_4 metals released under oxidizing conditions and clay minerals, and F_5 residual fraction)

	SFA3										SFA18									
	F_1		F_2		F_3		F_4		F_5		F_1		F_2		F_3		F_4		F_5	
	C_{ext}	RER	C_{ext}	RER	C_{ext}	RER	C_{ext}	RER	C_{ext}	RER	C_{ext}	RER	C_{ext}	RER	C_{ext}	RER	C_{ext}	RER	C_{ext}	RER
Ag	bdl	ND	1.3	54.51	0.0	ND	0.8	33.48	0.3	12.02	bdl	ND	1.8	47.67	bdl	ND	1.2	30.31	0.9	22.02
As	0.4	0.04	211.6	20.95	124.0	12.28	674.0	66.73	bdl	ND	0.7	0.05	242.3	17.69	190.0	13.87	937.0	68.39	bdl	ND
Cd	4.0	13.88	21.7	74.43	bdl	ND	0.3	1.03	3.1	10.65	1.9	10.33	11.7	64.81	1.5	8.29	0.8	4.42	2.2	12.15
Co	0.2	0.10	145.8	80.56	bdl	ND	26.0	14.36	9.0	4.97	0.2	0.21	73.4	73.39	3.4	3.40	15.5	15.50	7.5	7.50
Cr	0.1	0.05	25.3	12.16	8.0	3.85	117.6	56.54	57.0	27.40	0.1	0.06	21.1	11.79	12.2	6.82	120.6	67.37	25.0	13.97
Cu	3.3	0.37	491.7	54.88	1.0	0.11	313.0	34.93	87.0	9.71	3.2	0.32	489.8	49.52	35.0	3.54	356.0	36.00	105.0	10.62
Fe	3.0	0.00	6,517.0	8.28	bdl	ND	30,825.0	39.17	41,355.0	52.55	1.0	0.00	5,189.0	9.43	5,110.0	9.29	38,100.0	69.27	6,600.0	12.00
Mn	283.0	1.42	18,117.0	90.59	300.0	1.50	780.0	3.90	520.0	2.60	167.0	2.06	6,023.0	74.36	830.0	10.25	660.0	8.15	420.0	5.19
Ni	6.4	1.23	342.6	65.88	2.0	0.38	137.0	26.35	32.0	6.15	1.5	1.11	57.2	42.37	7.6	5.63	55.7	41.26	13.0	9.63
Pb	bdl	0.05	44.1	56.34	bdl	ND	16.1	20.59	18.0	23.02	bdl	ND	35.8	46.20	0.7	0.90	21.3	27.52	19.6	25.32
Sb	bdl	ND	0.4	10.57	bdl	ND	1.4	40.00	1.7	49.43	bdl	ND	0.2	3.50	bdl	0.32	1.5	27.07	3.9	69.11
Sn	bdl	ND	0,5	0,44	bdl	ND	38,5	34,38	73,5	65,63	bdl	ND	0,7	0,58	bdl	ND	53,3	44,42	66.0	55.00
W	bdl	ND	1.0	0,3.0	0,3	0,09	101,3	30,69	198,7	60,21	bdl	ND	0,6	0,10	0,4	0,07	199.0	33,61	392.0	66,22
Y	0.6	0.54	61.0	59.26	bdl	ND	15.2	14.76	26.2	25.44	bdl	0.31	0.6	47.94	0.5	2.27	2.8	19.97	8.1	29.50
Zn	74.0	2.78	2,156.0	81.05	bdl	ND	430.0	16.17	bdl	ND	10.0	1.03	496.0	51.03	54.0	5.56	351.0	36.11	61.0	6.28

bdl below detection limit, *ND* not determined

sulfates) in warm, dry periods. In contrast, such minerals are easily dissolved in rainy periods.

The highest percentage of Sn extraction is related to the last step of extraction in samples SFA3 and SFA18. These phases are highly resistant to both chemical and physical weathering and can be transported long distances from the source areas. According to Rose et al. (1979), the mobility of Sn in natural environments is dependent on low and high pH. Weathering induces the transport of natural and anthropogenic Sn under acidic and reducing conditions, SnS_2 is insoluble under reducing conditions (Brookins 1988).

These SCE results suggest that local wind and hydrological factors give rise to mechanisms of transport responsible for the dispersion of elements. The mechanical dispersion fuelled by the wind of hydrated metal sulfates, resulting from evaporation during warm period and stored in the open-air impoundments from Barroca Grande and Rio, induces the accumulation of these materials on solid materials such as soil. Also, these elements could be transported in suspension by surface waters or by acidic waters draining a number of sites, contaminating the soils with As and sulfide-related heavy metals (Cu, Pb, Zn, and Cd).

Conclusions

The mining and processing activities at Panasqueira mine produces arsenic-rich mine wastes that are largely responsible for the high levels of metals at the Barroca Grande and Rio tailings. Oxidation of sulfides may give rise to the mobilization and migration of trace metals from the mining wastes into the environment, releasing the contaminants to the ecosystems. The above referred As-rich mine wastes are the main source of pollution in the surrounding environment, namely in SFA soils.

The integrated procedure using PCA and CA allowed the authors to identify the contaminant group of elements associated to mining activities (As, Cd, Co, Cu, Mn, Ni, Sn, Y, W, and Zn were the elements of most concern) and the identification of sites that require intervention or remediation.

On other hand, it was possible to identify the elements that are responsible for the high degree of contamination and classify the quality of the local soil based on the estimation of the modified degree of contamination. According to the results obtained through a contamination factor determination, As and Zn are the variables that present very high contamination factors, leading to the fact that 65.4 % of the S. Francisco de Assis soil samples exhibit a moderate to high degree of pollution, and only 34.6 % of the samples were classified as nil to very low degree of pollution. The spatial distribution of this contamination factor shows that soils collected downstream Barroca Grande contain elements like As, Cd, Cu, Pb, and Zn, which occur in increased concentrations, when compared with local Bk soils. The mechanical dispersion, due to erosion, is the main factor fuelling this phenomenon. The practical results of this study allow selecting areas where an eventual remediation procedure may be foreseen. Priority should be given to areas where samples are classified as requiring reclamation, when they are geographically located in agricultural or urban areas.

An approach based on chemical sequential extraction demonstrates that the distribution/accumulation of trace metals in the SFA soils is, to a great extent, related to sulfides, but also to amorphous or poorly crystalline iron oxide geochemical phases. However, it was also noticed that a significant proportion of the As, Cd, Cu, and Zn is linked to exchangeable and acid-soluble species, upon which desorption and ion exchange reactions may originate the release of these readily mobile phases. These results disclose the fact that the wind and hydrological factors are fuelling the chemical elements transport mechanisms. Such factors are likely to be responsible for dispersion of the above referred elements, water being the main transporter medium and soils as one of the possible retention media.

Acknowledgments This research was funded by the European Commission through the e-Ecorisk Project (# EVG1-2002-25 0068) "*A regional enterprise network decision-support system for environmental risk and disaster management of large-scale industrial spills*". This research was financially supported by Fundação para a Ciência e Tecnologia (FCT), Quadro de Referência Estratégico Nacional (QREN), and Fundo Europeu de Desenvolvimento Regional (FEDER) (grants SFRH/BD/63349/2009 and SFRH/BPD/45884/2008).

References

Abrahim GMS, Parker RJ (2008) Assessment of heavy metal enrichment factors and the degree of contamination in marine sediments from Tamaki Estuary, Auckland, New Zealand. Environ Monit Assess 136:227–238

Adriano DC (1986) Trace elements in the terrestrial environment. Springer, New York

Andad–Multivariate Data Analysis Software. CVRM-IST, 2000.

Ávila P, Ferreira da Silva E, Salgueiro AR, Farinha JA (2008) Geochemistry and mineralogy of mill tailings impoundments from the Panasqueira mine (Portugal): implications for the surrounding environment. Mine Water Environ 27:210–224

Benvenuti M, Mascaro I, Corsini F, Lattanzi P, Parrini P, Tanelli G (1995) Mine waste dumps and heavy metal pollution in abandoned mining district of Boccheggiano southern Tuscany, Italy. Environ Geol 30:238–243

Breiter K (2001) Report about Laboratory Investigations of Rock Samples from the Panasqueira Mine and Recommendations for Future Exploration, Nov 2001.

Brookins DG (1988) E_h–pH diagrams for geochemistry. Springer, Berlin, Germany

Cavey G, Gunning D (2006) Updated technical report on the Panasqueira mine, Distrito de Castelo Branco. Portugal, OREQUEST

CCME–Canadian Council of Ministers of the Environment (1999) Canadian soil quality guidelines for the protection of environmental

and human health. Canadian Council of Ministers of the Environment, Winnipeg
Chapman BM, Jones DR, Jung RF (1983) Processes controlling metal ion attenuation in acid mine drainage streams. Geochim Cosmochim Ac 47:1957–1973
Chon HT, Cho CH, Kim KW, Moon HS (1995) The occurrence and dispersion of potentially toxic elements in areas covered with black shales and slates in Korea. Appl Geochem 11:69–76
Correa A, Naique RA (1998) Minas Panasqueira, 100 years of mining history paper presented at the 1998 International Tungsten Industry Association (ITIA) conference.
Corrêa de Sá A, Naique RA, Nobre E (1999) Minas da Panasqueira—100 anos de História. Bol de Minas 36(1):3–22
Davis JC (1986) Statistics and data analysis in geology, 2nd ed. Wiley, New York
Deschamps E, Ciminelli VST, Lange FT, Matschullat J, Raue B, Schmidt H (2002) Soil and sediment geochemistry of the Iron Quadrangle, Brazil: the case of arsenic. J Soils Sediments 2 (4):216–222
e-Ecorisk (2007) A regional enterprise network decision-support system for environmental risk and disaster management of large-scale industrial spills. WP3—case study characterisation. Deliverable 3.1.
Einax JW, Soldt U (1999) Geostatistical and multivariate statistical method for the assessment of polluted soils; merits and limitations. Chemometr Intell Lab:79–91.
Ellickson KM, Meeker RJ, Gallo MA, Buckley BT, Lioy PJ (2001) Oral bioavailability of lead and arsenic from a NIST standard reference soil material. Arch Environ Con Tox 40:128–135
Ferreira da Silva E, Matos JX, Patinha C, Reis P, Cardoso Fonseca E (2005) The effect of unconfined mine tailings on the geochemistry of soils, sediments and surface waters of the Lousal area (Iberian Pyrite Belt, Southern Portugal). Land Degrad Dev:213–228
Ferreira MMSI (2004) Dados geoquímicos de base de solos de Portugal Continental, utilizando amostragem de baixa densidade. Tese de Doutoramento da Universidade de Aveiro.
Galán E, Gómez-Ariza JL, González I, Fernández-Caliani JC, Morales E, Giráldez I (2003) Heavy metal partitioning in river sediments severely polluted by acid mine drainage in the Iberian Pyrite Belt. Appl Geochem 18:409–421
geoMS–Geostatiscal Modelling Software. CMRP-IST, 2000.
Godin P (1983) Les sources de pollution des sols: Essai de quantification des risques associés aux éléments traces (Sources of pollution of the soils: test of quantification of the risks due to the elements traces). Sci Sol 2:73–87
Goovaerts P (1997) Geostatistics for natural resources evaluation. Oxford University Press
Gray NF (1997) Environmental impact and remediation of acid mine drainage: a management problem. Environ Geol 30:62–71
Greenacre MJ (1984) Theory and applications of correspondence analysis. Academic Press, London
Hakanson L (1980) Ecological risk index for aquatic pollution control, a sedimentological approach. Water Res 14:975–1001
Henin S (1983) Les éléments en traces dans le sol (Trace elements in the soil). Sci Sol 2:67–71
Jung MC (2001) Heavy metal contamination of soils and waters in and around the Imcheon Au–Ag mine, Korea. Appl Geochem 16:1369–1375
Kelly WC, Rye RO (1979) Geologic, fluid inclusion and stable isotope studies of the tin–tungsten deposits of Panasqueira, Portugal. Econ Geol 74:1721–1822
Kim KW, Lee HK, Yoo BC (1998) The environmental impact of gold mines in the Yugu-Kwangcheon Au–Ag metallogenic province, Republic of Korea. Environ Technol 19:291–298
Kloke A (1979) Contents of arsenic, cadmium, chromium, fluorine, lead, mercury, and nickel in plants grown on contaminated soil. UN-ECE Symposium, Geneva
Lee CG, Chon HT, Jung MC (2001) Heavy metal contamination in the vicinity of the Daduk Au-Ag-Pb-Zn mine in Korea. Appl Geochem 16:1377–1386
Liu WX, Coveney RM, Chen JL (2003) Environmental quality assessment on a river system polluted by mining activities. Appl Geochem 18:749–764
Liu WH, Zhao JZ, Ouyang ZY, Solderland L, Liu GH (2005) Impacts of sewage irrigation on heavy metal distribution and contamination in Beijing, China. Environ Intl 31(6):805–812
Manly BFJ (1994) Multivariate statistical methods: a primer, 2nd edn. Chapman and Hall, Boca Raton
Massart DL, Kaufman L (1983) The interpretation of analytical chemical data by the use of cluster analysis. Wiley, New York, 65
McKenzie AB, Pulford ID (2002) Investigation of contaminant metal dispersal from a disused mine site at Tyndrum, Scotland, using concentration gradient and Pb isotope ratios. Appl Geochem 17:1093–1103
Nishida H, Miyai M, Tada F, Suzuki S (1982) Computation of the index of pollution caused by heavy metals in river sediments. Environ Poll (séries B) 4:241–248
Nordstrom DK (1982) The effect of sulfate on aluminum concentrations in natural waters: some stability relations in the system Al_2O_3–SO_3–H_2O at 298 K. Geochim Cosmochim Ac 46:681–692
Noronha F, Doria A, Dubessy J, Charoy B (1992) Characterization and timing of the different types of fluids present in the barren and ore veins of the W-Sn deposit of Panasqueira, Central Portugal. Miner Deposita 27:72–79
Pickering WF (1986) Metal ion speciation – soils and sediment. Ore Geol Rev 1:83–146
Radojevic M, Bashkin VN (1999) Practical environmental analysis. The Royal Society of Chemistry, Cambridge
Reimann C, De Caritat P (1998) Chemical elements in the environment: factsheets for the geochemist and environmental scientist. Springer, Berlin
Rose AW, Hawkes HE, Webb JS (1979) Geochemistry in mineral exploration, 2nd ed. Academic Press, London, UK
Smith M (2006) Panasqueira the tungsten giant at 100+. Operation Focus Int Mining 2:10–14
Son HO, Jung MC (2011) Relative extraction ratio (RER) for arsenic and heavy metals in soils and tailings from various metal mines, Korea. Environ Geochem Hlth 33:121–132. doi:10.1007/s10653-010-9356-0
Tessier A, Campbell PGC, Bisson M (1979) Sequential extraction procedure for the speciation of particulate trace metals. Anal Chem 51(7):844–851
Verner JF, Ramsey MH (1996) Heavy metal contamination of soils around a Pb-Zn smelter in Bukowno, Poland. Appl Geochem 11 (1–2):11–16
Wackernagel H (1998) Multivariate geostatistics: an introduction with applications, 2nd edn. Springer, Berlin
Witte KM, Wanty RB, Ridley WI (2004) Engelmann Spruce (*Picea engelmanni*) as a biological monitor of changes in soil metal loading related to pas mining activities. Appl Geochem 19:1367–1376
Wong SC, Li XD, Zhang G, Qi SH, Min YS (2002) Heavy metals in agricultural soils of Pearl River Delta, South China. Environm Pollut 119:33–44
Yan X-P, Kerrich R, Hendry MJ (1999) Sequential leachates of multiple grain size fractions from a clay-rich till, Sakatchewan, Canada: implications for control on the rare earth element geochemistry of pore waters in an aquitard. Chem Geol 158:53–79
Zhou JM, Dang Z, Cai MF, Liu CQ (2007) Soil heavy metal pollution around the Dabaoshan Mine, Guangdong Province, China. Pedosphere 17(5):588–594